第 31 卷第 2 期
2015 年 2 月

无 机 化 学 学 报
CHINESE JOURNAL OF INORGANIC CHEMISTRY

Vol.31 No.2
361-368

一种应用于活细胞中检测 Hg(Ⅱ)的苯并噻唑类荧光探针

焦元红[1,3] 张 前[1] 姜玉凤[1] 张万举*[,2]

([1]湖北理工学院化学与化工学院,黄石 435003)

([2]催化材料制备及应用湖北省重点实验室,黄冈师范学院,黄冈 438000)

([3]矿区环境污染控制与修复湖北省重点实验室,湖北理工学院,黄石 435003)

摘要:合成和表征了一种苯并噻唑类的荧光探针(YH1),并用光谱法研究了它对不同金属离子的响应。结果表明:YH1 对 Hg^{2+}显示出好的选择性和灵敏度,与 Hg^{2+}作用后,在紫外光的激发下它的溶液颜色由蓝色变为无色。在 1.4~8.8 μmol·L^{-1} 浓度的范围内,YH1 的荧光强度与 Hg^{2+}浓度有线性关系,其对 Hg^{2+}的检出限为 0.56 μmol·L^{-1}。此外,YH1 可跨过细胞膜,细胞毒性低,还可应用于 HeLa 活细胞中对 Hg^{2+}进行荧光成像。

关键词:晶体结构;汞离子;荧光探针;苯并噻唑;荧光成像

中图分类号:O614.24+3 **文献标识码**:A **文章编号**:1001-4861(2015)02-0361-08

DOI:10.11862/CJIC.2015.019

A Benzothiazole-Derived Fluorescent Probe for Detecting Hg(Ⅱ) in Live Cells

JIAO Yuan-Hong[1,3] ZHANG Qian[1] JIANG Yu-Feng[1] ZHANG Wan-Ju*[,2]

([1]*College of Chemistry and Chemical Engineering, Hubei Polytechnic University, Huangshi, Hubei* 435003, *China*)

([2]*Hubei Key Laboratory for Processing and Application of Catalytic Materials, Huanggang Normal University, Huanggang, Hubei* 438000, *China*)

([3]*Hubei Key Laboratory of Mine Environmental Pollution Control & Remediation, Hubei Polytechnic University, Huangshi, Hubei* 435003, *China*)

Abstract: A benzothiazole-derived fluorescent probe (YH1) has been synthesized and structurally characterized, and its response to different metal ions has been investigated by spectrometry. The results showed that YH1 exhibited good sensitivity and selectivity to Hg^{2+}. Its interaction with Hg^{2+} caused the color of its solution changed from blue to colorless under UV irradiation. There was a good linear relationship between the fluorescence intensity of YH1 and the concentration of Hg^{2+} in the range of 1.4 μmol·L^{-1} to 8.8 μmol·L^{-1}, and its detection limit for Hg^{2+} was 0.56 μmol·L^{-1}. Moreover, the cell membrane penetration of YH1 had low cytotoxicity, and it can be applied to image intracellular Hg^{2+} in living HeLa cells. CCDC: 978108.

Key words: crystal structure; Hg^{2+}; fluorescent probe; benzothiazole; fluorescent imaging

Heavy metals have attracted considerable attention because of their wide use and subsequent impact on the environment and human health. One of the very toxic and frequently used heavy metals is mercury. Hg^{2+} has been well known as an environmental pollutant for several decades, and it damages DNA, impairs

收稿日期:2014-08-29。收修改稿日期:2014-10-25。

湖北省教育厅 B 类项目(No.B20114404),矿区环境污染控制与修复湖北省重点实验室开放基金项目(No.2012103)和湖北省教育厅青年人才资助项目(No.Q20132901)。

*通讯联系人。E-mail:zhangwanju2014@163.com

mitosis, and disrupts the central nervous and endocrine systems[1]. So the detection and quantification of Hg^{2+} is important.

Fluorescent probes are indispensable tools for visualizing ions at the molecular level without the need for special instrumentation because of their simplicity, rapidity, convenience and selectivity in fluorescence assays[2-3]. In recent years, numerous fluorescent probes for Hg^{2+} have been extensively explored by combining an appropriate fluorophore with the receptor as a metal ion recognition moiety. Different fluorophores of these probes mainly focused on rhodamine, fluorescein, coumarin, cyanine, iridium(Ⅲ) complex, boron-dipyrromethene (BODIPY), dansyl, naphthalene, 7-nitrobenz-2-oxa-1,3-diazole (NBD) and others[4-15]. The metal ion receptor including cyclam, diazatetrathia crown ether, 3,6,12,15-tetrathia-9-azaheptadecan have been successfully utilized for the selective detection of Hg^{2+} [16-18]. However, the development of a high selective and sensitive fluorescent probe for Hg^{2+} is still a challenge. Benzothiazole is often taken as a fluorophore for designing fluorescence probes to detect metal ions due to its good photophysic properties[19-20]. Considering the strong affinity of mercury to sulfur, we designed a benzothiazole-derived fluorescent probe containing sulfur atoms, and its synthesis, crystal structure, fluorescent properties and application were reported in this paper.

1 Experimental

All reagents were purchased from commercial companies and directly used unless stated otherwise. The melting point was determined with an XT4A micromelting point apparatus and was uncorrected. Elemental analyses were carried out on a Perkin-Elmer 2400 instrument. Fluorescence spectra were performed on a FluoroMax-P spectrofluorimeter. UV-Vis spectra were recorded on an Analytik jena Specord 210 spectrophotometer. ^{1}H NMR spectra were recorded on a Varian Mercury 400 spectrometer at 400 MHz. Electrospray ionization mass spectra (ESI-MS) were acquired on an Applied Biosystems API 2000 LC/MS/MS system. Live-Cell Imaging was performed on Leica DMI 3000B fluorescent inverted microscope.

1.1 Synthesis of the probe YH1

The starting material (**1**) was synthesized according to the procedure previously described, which was further treated as follows to afford probe YH1 (Scheme 1)[21]. Sodium filings (0.46 g, 0.02 mol) were dissolved in EtOH. Ethanethiol (0.62 g, 0.01 mol) was added to the above solution and the mixture was stirred at room temperature for 1 h. Then the intermediate **1** (1.75 g, 0.005 mol) was added and the mixture was refluxed for 24 h. After the reaction was completed, the solvent was evaporated in vacuo and then 100 mL of water was added to the residue. The aqueous solution was extracted with CH_2Cl_2 (100 mL×3). The extract was dried over $MgSO_4$. After removal of the solvent, the residue was purified by flash chromatography (silica, petroleum ether/AcOEt, 5:1, *V*/*V*) to give a yellow compound YH1. Yield: 75%; m.p. 71.6~72.5 °C. ^{1}H NMR (400 MHz, $CDCl_3$): δ 7.83~7.99 (m, 4H), 7.26~7.44 (m, 2H), 6.85 (d, *J*=8.4 Hz, 2H), 3.62 (t, *J*=7.6 Hz, 4H), 2.77 (t, *J*=7.8 Hz, 4H), 2.62 (q, *J*=7.2 Hz, 4H). 1.30(t, *J*=7.6 Hz, 6H). ESI-MS: *m*/*z*: 403.8 $[M+H]^+$. Anal. Calcd. for $C_{21}H_{26}N_2S_3$ (%): C, 62.64; H, 6.51; N, 6.96; Found(%): C, 62.34; H, 6.75; N, 6.88.

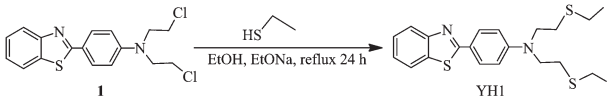

Scheme 1 Synthesis of the probe YH1

1.2 X-ray crystallography

Yellow crystals of the probe YH1 having approximate dimensions of 0.30 mm ×0.30 mm×0.20 mm was mounted on a glass fiber in a random orientation at 298(2) K. The determination of unit cell and the data collection were performed with Mo *Kα* radiation (λ=0.071 069 nm) on a Bruker Smart APEX-CCD diffact-ometer with φ-ω scan mode. A total of 8 266 reflec-tions were collected in the range of $2.04°<\theta<25.05°$ at room temperature. The structures were solved by direct methods and semiempirical absorption correc-tions were applied. The nonhydrogen atoms were located by direct phase determination and full-matrix least-squares refinement on F^2, while the

hydrogen atoms for non-water protons were treated using the riding mode. The -$CH_2CH_2SCH_2CH_3$ groups were disordered over two sites with different occupancies, for example, C14, C15 with 0.823 and C14′, C15′ with 0.177. The distances of the C-C and C-S bonds were constrained by using parameters from the similar structure. The final cycle of full matrix least-squares refinement was based on 3 731 independent reflections [$I>2\sigma(I)$]. All calculations were carried out on a PC using SHELXS-97 and SHELXL-97 programs[22-23]. Crystal data and structural refinement were summarized in Table 1. The selected bond lengths and bond angles were listed in Table 2, and the hydrogen bond lengths and bond angles were given in Table 3.

CCDC: 978108.

Table 1　Crystal data and structure refinements of the probe YH1

Formula	$C_{21}H_{26}N_2S_3$	γ / (°)	93.880(3)
Formula weight	402.62	V / nm^3	1.075 3(4)
Temperature / K	298(2)	Z	2
Crystal size / mm	0.30×0.30×0.20	D_c / (g·cm^{-3})	1.244
Crystal system	Triclinic	F(000)	428
Space group	$P\bar{1}$	Reflections collected / unique	8 266/ 3 731
a / nm	0.982 8(2)	R_{int}	0.023 2
b / nm	1.006 4(2)	Data / restrains / parameters	3 731 / 96 / 323
c / nm	1.105 8(2)	Final R indices [$I>2\sigma(I)$]	R_1=0.064 2, wR_2=0.168 8
α / (°)	94.363(3)	R indices (all data)	R_1=0.085 1, wR_2=0.181 6
β / (°)	98.458(2)	GOF on F^2	0.985

Table 2　Selected bond lengths (nm) and bond angles (°) of the probe YH1

S(1)-C(6)	0.173 2(3)	S(1)-C(7)	0.175 4(3)	N(1)-C(7)	0.129 6(4)
N(1)-C(1)	0.138 5(4)	C(8)-C(13)	0.138 5(4)	C(8)-C(9)	0.138 8(4)
C(7)-N(1)-C(1)	111.6(2)	N(1)-C(1)-C(2)	125.3(3)	C(14)-N(2)-C(16)	114.5(3)

Table 3　Hydrogen bond lengths (nm) and bond angles (°)

D–H…A	d(D-H)	d(H…A)	d(D…A)	∠DHA
Intra C(9)–H(9)…N(1)	0.093	0.259	0.289 9(4)	100
Intra C(13)–H(13)…S(1)	0.093	0.272	0.313 4(3)	108

1.3　Fluorescent response experiment

A stock solution of YH1 was prepared by dissolution in ethanol/water (1:1, V/V). The solutions of different metal ions (K^+, Ca^{2+}, Na^+, Mg^{2+}, Mn^{2+}, Fe^{2+}, Fe^{3+}, Co^{2+}, Ni^{2+}, Cu^{2+}, Zn^{2+}, Cd^{2+}, Hg^{2+}) were dissolved in deionized water (1 mmol·L^{-1}). Fluorescence titration was performed on 2 mL solution of YH1 in a quartz cell, by adding different stock solutions of cations into the quartz cell each time. After mixing well, the fluorescence spectrum of the solution was recorded. All of the spectroscopic measurements were carried out in Tris-HCl buffer (20 mmol·L^{-1}, pH 7.4) at room temperature.

1.4 Fluorescent imaging of Hg^{2+}

HeLa cells were seeded in a 24-well plate in culture media (1:1, V/V) mixture of Dulbecco′s modified Eagle′s medium and Ham′s F-12 (Invitrogen) supplemented with 12.5% fetal bovine serum) for 24 h before imaging. On the day of experimentation, cells were rinsed twice with phosphate buffered saline (PBS) and incubated with YH1 (2 μmol·L^{-1}) for 30 min. Prior to imaging, cells were again rinsed twice with PBS to remove the remaining probe, the cells were further treated with 20 μmol·L^{-1} $Hg(ClO_4)_2$ for 30 min. The treated cells were imaged by inverted fluorescence microscopy with a 40× objective lens

(excited with green light). For all images, the microscopy settings, such as brightness and contrast were held constant to compare the relative intensity of intracellular YH1 fluorescence.

1.5 Cytotoxicity assay

The cytotoxicity of probe YH1 was assessed by MTT assay. The HeLa cells supplemented with 10% FBS, 100 U·mL^{-1} of penicillin, and 100 U·mL^{-1} of streptomycin were seeded at about 1 000~10 000 cells per well (200 μL) in 96-well plates, and incubated at 37 ℃ in a 5% CO_2 humidified air atmosphere. After 24 h of incubation in the medium, the wells were divided into one experimental group and one control group. The experimental group was added to 2 μmol·L^{-1} YH1 and incubated for 12 h or 24 h. Then, after removing the medium, 20 μL of MTT (5 mg·mL^{-1}) in PBS was added to wells. After incubation of 4 h, the MTT-containing medium was replaced by DMSO of 150 μL. Finally, the 96-well plates were oscillated for 10 min to fully dissolve the formazan crystal formed by living cells in the wells. The relative viability of the cells in each well was produced by absorbance of at 490 nm each well determined with the Biotek Synergy™ 2 Multi-detection Microplate Reader.

2 Results and discussion

2.1 Crystal structure of the probe YH1

Yellow crystals of the probe YH1 were obtained by slow evaporation of a dichloromethane solution at room temperature. In the crystal structure (Fig.1), the benzothiazole ring system and adjacent benzene ring constitute the fluorescent moiety of the probe YH1, they are nearly coplanar, and their dihedral angle is 3.00(2)°. The N1-C7 (0.129 6(4) nm) bond indicates double-bond character, whereas the S-C bond lengths are indicative of significant single-bond character. The S1-C6 (0.173 2(3) nm) bond is shorter than S1-C7 (0.175 4(3) nm), due to the fact that C7 is sp^2 hybridized, whereas C6 is part of the aromatic ring (Table 2). N2, S2, S3 are coordination atoms of chelating moiety, two torsion angles (N2-C16-C17-S3 and N2-C14-C15-S2) are 177.19° and 179.21°, respectively. The angle of C16-N2-C14 is 114.5(3)°, which leads to Y-shape of the whole molecule. As shown in Table 3 and Fig. 2, the molecules are stablized by intramolecular C–H ⋯ N and C–H ⋯ S hydrogen bonds, leading to the formation of a three dimension network.

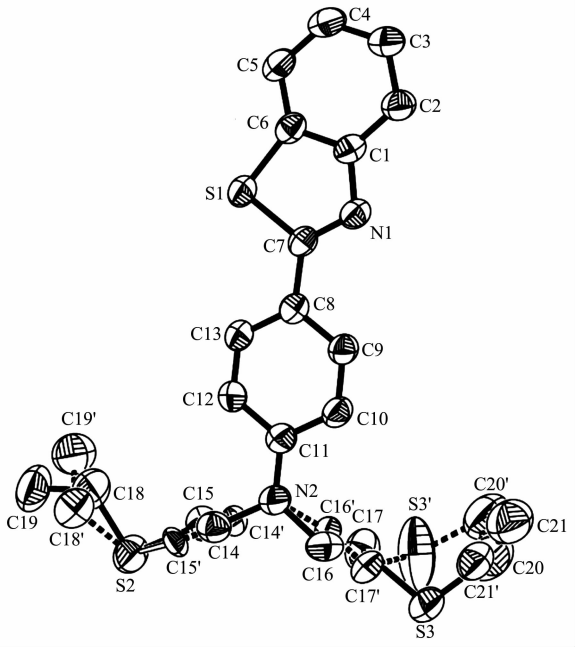

Ellipsoids are at the probability level of 30%, and the hydrogen atoms are omitted for clarity

Fig.1 ORTEP view of structure of the probe YH1

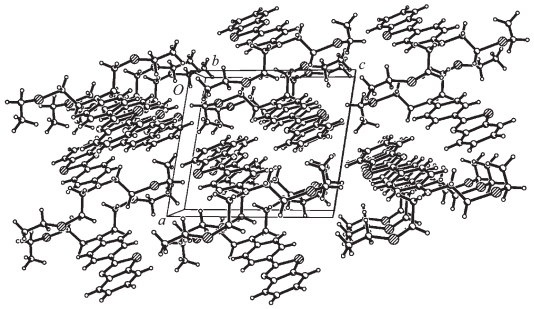

Fig.2 Packing of the probe YH1 in unit cell

2.2 Response of YH1 to Hg^{2+}

The spectral properties of YH1(10 μmol·L^{-1}) was evaluated in the mixed solvents of ethanol/water (1:1, *V*/*V*). Studies on the UV-Vis absorption of YH1 revealed that a strong absorption band centered around 330 nm, and the maximum absorption wavelength was unchanged on addition of Hg^{2+} (Fig.3). The maximum excitation (λ_{ex}) and emission (λ_{em}) wavelengths of YH1 were measured to be 335 and 425 nm, respectively. To obtain insight into the interactions of YH1 toward various metal ions (K^+,

Ca^{2+}, Na^{+}, Mg^{2+}, Mn^{2+}, Fe^{2+}, Fe^{3+}, Co^{2+}, Ni^{2+}, Cu^{2+}, Zn^{2+}, Cd^{2+}, Hg^{2+}), its chemosensing behavior with metal ions (2 equiv.) was investigated by fluorescence spectroscopy (Fig.4). It′s found that YH1 showed a remarkable fluorescence quenching in presence of Hg^{2+}, and about 20% decrease in fluorescence intensity was observed upon the addition of Cu^{2+}, while other metal ions revealed almost negligible effect on the fluorescence behavior of YH1. The result indicated that YH1 was highly selective to Hg^{2+}. Metal ions competition experiments were carried out to test practical applicability of YH1 as a chemoprobe for Hg^{2+}. As shown in Fig.5, YH1 (10 μmol·L^{-1}) exhibited a selective signaling behavior toward 1 equiv. of Hg^{2+} in the presence of 100 equiv. of other common metal ions. It′s obvious that the background metal ions did not significantly interfere in the response of Hg^{2+}. So YH1 could be used as a potential Hg^{2+}-selective fluorescent probe in the presence of physiologically important metal ions.

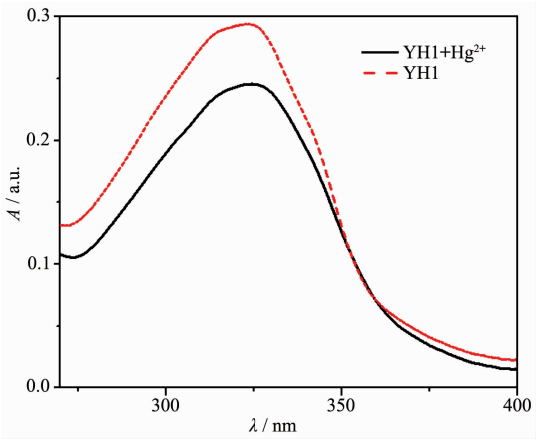

Fig.3　Change in UV spectra of YH1 upon interaction with Hg^{2+}

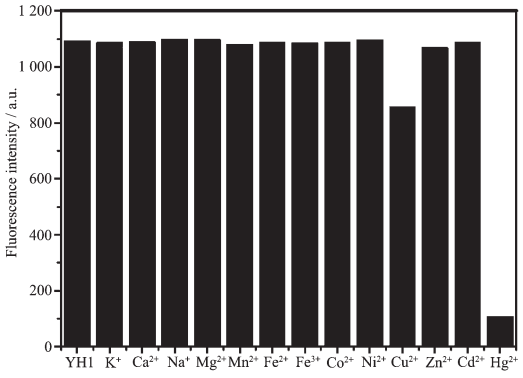

Fig.4　Fluorescent response of YH1 (10 μmol·L^{-1}) to various metal ions (10 μmol·L^{-1}) in CH_3CH_2OH/Tris-HCl buffer (1:1, *V*/*V*, pH 7.4)

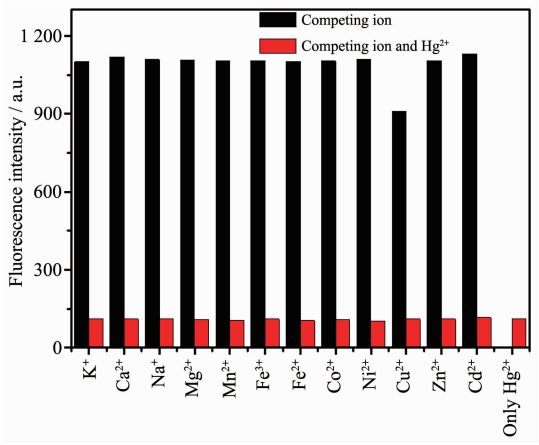

Fig.5　Effect of Hg^{2+} on YH1 (10 μmol·L^{-1}) in the presence of different metal ions (1 mmol·L^{-1})

To examine the sensitivity toward Hg^{2+}, YH1 was titrated against Hg^{2+} in EtOH/Tris-HCl buffer (1:1, *V*/*V*, pH 7.4). Upon addition of increasing amounts of Hg^{2+}, the emission intensity at 425 nm decreased slowly (Fig.6). With 2 equiv. of Hg^{2+}, the fluorescence of YH1 was nearly completely quenched. The “on-off” fluorescence changes of YH1 to Hg^{2+} were also illustrated in the inset photograph (Fig.6). After the addition of 2 equiv. of Hg^{2+} to the YH1 solution, a significant fluorescence color change (from bright blue to colorless) can be easily observed by naked eyes under the irradiation at 365 nm. There was a good linear relationship (linear correlation coefficient R^2=

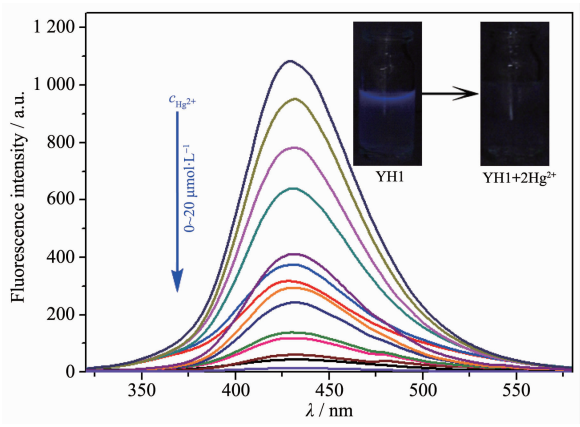

Inset: YH1 (10 μmol·L^{-1}) in the absence and presence of Hg^{2+} under UV light (365 nm)

Fig.6　Emission intensity of YH1 (10 μmol·L^{-1}) changes with increasing concentrations of Hg^{2+} (0~20 μmol·L^{-1})

0.989 3) between the fluorescence intensity of YH1 and the concentration of Hg^{2+} in the range of 1.4~8.8 μmol·L^{-1} (Fig.7). The detection limit of YH1 to Hg^{2+} was determined to be 0.56 μmol·L^{-1} according to the calculation method reported in the literature [24]. The fluorescence spectrum of YH1 in response to different pH value was also investigated (Fig.8). The fluorescence of YH1 was nearly stable in a wide pH value range of 2~12, however, upon addition of Hg^{2+}, it remained unchanged with increasing pH value from 5 to 9. These two pH ranges were both good for imaging Hg^{2+} at around pH 7 and in biological media. Moreover, the stoichiometry of interactions between YH1 and Hg^{2+} was studied by the Job′s plot experiment, where the emission changes at 425 nm were plotted against molar fractions of YH1 under the conditions of an invariant total concentration (10 μmol·L^{-1}). As a result, when the molar fraction of $c_{YH1}/(c_{YH1}+c_{Hg^{2+}})$ was about 0.67, the change of emission approached a maximum (Fig.9), indicating the 2∶1 stoichiometry for the YH1-Hg^{2+} complex. Based on 2∶1 stoichiometry, the association constant for the complex formation between YH1 and Hg^{2+} was calculated to be 8.24×10^6 L^2·mol^{-2} by using Benesi-Hildebrand equation[25].

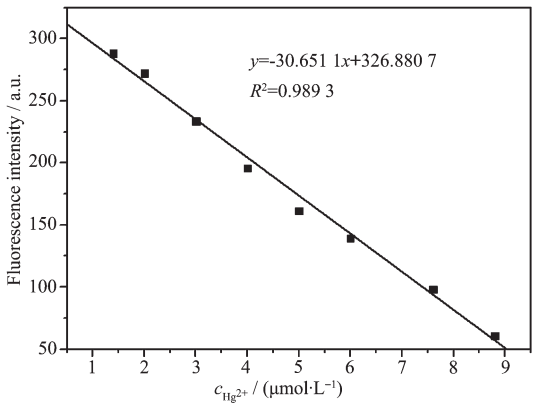

Fig.7 Fluorescence intensity of YH1 as a function of concentration of Hg^{2+} (1.4~8.8 μmol·L^{-1})

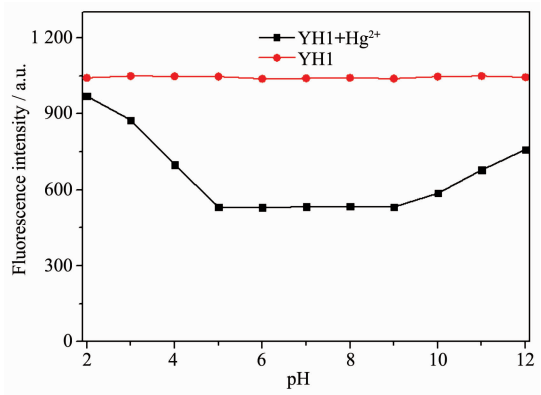

Fig.8 Fluorescence intensity of YH1 (10 μmol·L^{-1}) and YH1+Hg^{2+} over a pH value range of 2~12 at room temperature

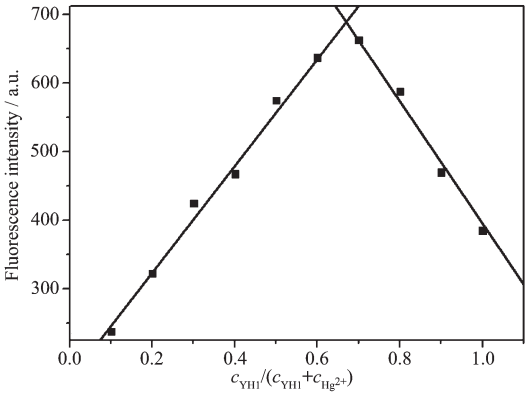

Fig.9 Job′s plot of interaction between Hg^{2+} and YH1 ($c_{YH1}+c_{Hg^{2+}}$=10 μmol·L^{-1})

According to above results and some reports, a possible complexation mechanism seemed to be reasonable for the binding site of YH1 with Hg^{2+} [14,26]. In the chelating moiety of YH1, there were two sulfur atoms and one nitrogen atom, which probably formed a suitable binding site for Hg^{2+}. When Hg^{2+} was added, the sulfur and nitrogen atoms donated their lone pair of electrons to the empty orbital of Hg^{2+}. The observed fluorescence quenching upon interaction with Hg^{2+} was probably due to the electron or energy transfer between the chelating unit and the benzothiazole fluorophore. Therefore, we propose that the reaction of YH1 with Hg^{2+} would yield the 2∶1 complex, as depicted in Scheme 2.

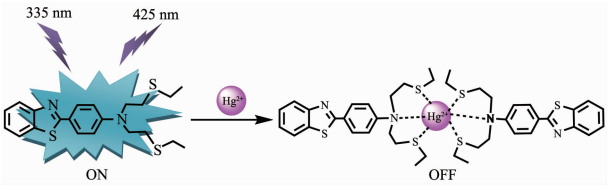

Scheme 2 Proposed binding model of YH1 with Hg^{2+}

2.3 Imaging of Hg^{2+} and cytotoxicity of YH1

The usefulness of YH1 for fluorescence imaging of Hg^{2+} was tested in living HeLa cells. When HeLa cells were only incubated with YH1 (2 μmol·L^{-1}) in

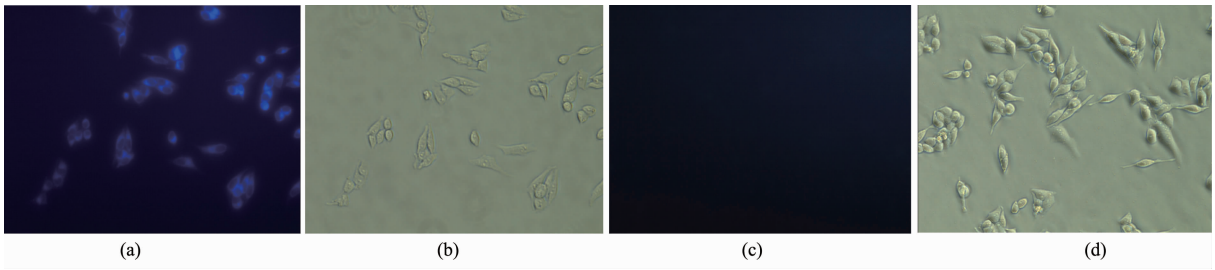

Fig.10　Fluorescence images of HeLa cells treated with YH1: (a) HeLa cells incubated with 2 μmol·L^{-1} YH1 for 30 min at 37 °C; (b) the bright-field images of HeLa cells from (a); (c) HeLa cells from (a) 30 min after treatment with 20 μmol·L^{-1} Hg^{2+}; (d) the bright-field images of HeLa cells from (c)

PBS for 30 min at 37 ℃, YH1 was found to be shown strong blue fluorescence, indicating that it can permeate into the cells and accumulate in them (Fig. 10a). However, no intracellular fluorescence was observed when the above cells treated with YH1 were further incubated with 20 μmol·L^{-1} Hg^{2+} for 30 min (Fig.10c). The notable decrease observed in intracellular fluorescence was due to the interaction between YH1 and Hg^{2+}. Further bright-field measurements confirmed that the cells were viable throughout the imaging experiments (Fig.10b, 10d). Thus, it can be said that YH1 might be a useful molecular probe for studying biological processes involving Hg^{2+} within living cells.

The cytotoxicity of the probe is an important aspect in the biological application. We also investigated the cytotoxicity of YH1 in living HeLa cells using MTT assay (Fig.11). The results showed that cell viability was 97% or 95% when HeLa cells were incubated with YH1(2 μmol·L^{-1}) for 12 h or 24 h. So YH1 had low cytotoxicity, and it might be suitable for the long-time detection of intracellular Hg^{2+}.

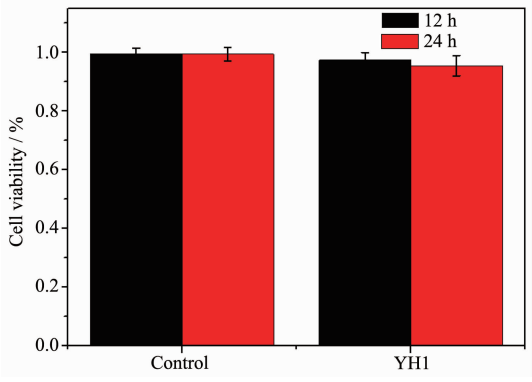

Fig.11　Cytotoxicity of probe YH1 (2 μmol·L^{-1}) in living HeLa cells for 12 h or 24 h

3　Conclusions

In conclusion, we prepared a benzothiazole-derived fluorescent probe YH1 for Hg^{2+}, which was characterized by single crystal X-ray diffraction. YH1 was sensitive and selective to Hg^{2+}, even in excess other interference metal ions. Under UV irradiation, the color of YH1 solution changed from blue to colorless upon addition of Hg^{2+}. The practical applications in living Hela cells inferred the ability of YH1 could detect intracelluar Hg^{2+}, indicating that YH1 has great prospective for detecting Hg^{2+} in bioanalytical assays.

References:

[1] Nolan E M, Lipard S J. *Chem. Rev.*, **2008**,**108**:3443-3480

[2] Guo Z Q, Park S, Yoon J, et al. *Chem. Soc. Rev.*, **2014**,**43**:16-29

[3] Li X H, Gao X H, Shi W, et al. *Chem. Rev.*, **2014**,**114**:590-659

[4] Guo Z Q, Zhu W H, Zhu M M, et al. *Chem. Eur. J.*, **2010**, **16**:14424-14432

[5] Tong S, Zhang L, Bing L, et al. *Sensor Actuators B*: *Chem.*, **2014**,**203**:157-164

[6] Nolan E M, Racine M E, Lippard S J. *Inorg. Chem.*, **2006**, **45**:2742-2749

[7] Shi H F, Liu S J, Sun H B, et al. *Chem. Eur. J.*, **2010**,**16**:12158-12167

[8] Tsukamoto K, Shinohara Y, Iwasakia S, et al. *Chem. Commun.*, **2011**,**47**:5073-5075

[9] Zhao Q, Liu S J, Li F Y, et al. *Dalton Trans.*, **2008**:3836-3840

[10]Tayade K, Bondhopadhyay B, Basu A, et al. *Talanta*, **2014**, **122**:16-22

[11]Sun H B, Liu S J, Ma T C, et al. *New J. Chem.*, **2011**,**35**:

1194-1197

[12]Wanichacheva N, Watpathomsub S, Lee V S, et al. *Molecules*, **2010**,**15**:1798-1810

[13]Zhao Q, Cao T Y, Li F Y, et al. *Organometallics*, **2007**,**26**:2077-2081

[14]Jeong H J, Li Y, Hyun M H. *Bull. Korean Chem. Soc.*, **2011**,**32**:2809-2812

[15]Tsukamoto K, Shinohara Y, Iwasakia S, et al. *Chem. Commun.*, **2011**,**47**:5073-5075

[16]Kim S H, Kim J S, Park S M, et al. *Org. Lett.*, **2006**,**8**:371-374

[17]Kim S H, Youn N J, Park J Y, et al. *Bull. Korean Chem. Soc.*, **2006**,**27**:1553-1156

[18]Sakamoto H, Ishikawa J, Nakao S, et al. *Chem. Commun.*, **2000**:2395-2396

[19]Santra M, Roy B, Ahn K H. *Org. Lett.*, **2011**,**13**:3422-3425

[20]Sun W, Li W H, Li J, et al. *Tetrahedron Lett.*, **2012**,**53**:2332-2335

[21]ZHANG Yong(张勇), WANG Qiang(王强), LI Wei(李伟), et al. *Chin. J. Org. Chem.*(有机化学), **2014**,**34**(2):403-408

[22]Sheldrick G M. *SHELXS*-97, *Program for the Solution of Crystal Structures*, University of Göttingen, Germany, **1997**.

[23]Sheldrick G M. *SHELXL*-97, *Program for the Refinement of Crystal Structures*, University of Göttingen, Germany, **1997**.

[24]Shortreed M, Kopelman R, Kuhn M, et al. *Anal. Chem.*, **1996**,**68**:1414-1418

[25]Benesi H A, Hildebrand J H. *J. Am. Chem. Soc.*, **1949**,**71**:2703-2707

[26]Jeong H J, Li Y, Hyun M H. *Bull. Korean Chem. Soc.*, **2011**,**32**:2809-2812